72nd International Astronautical Congress (IAC), Dubai, United Arab Emirates, 25-29 October 2021.

IAC-21,B4,7,3,x66544

Multi-CubeSat Mission for Auroral Acceleration Region Studies

M. Castro[a]*, L. Felicetti[b], S. Sadeghi[a], S. Satpute [a], V. Barabash[a], E. Jeronimo de Oliveira [a], L.G. Westerberg[c], R.Laufer[a]

[a] Department of Computer Science, Electrical and Space Engineering, *Luleå University of Technology*, 98128 Kiruna, Sweden, marley.s.castro@gmail.com
[b] School of Aerospace Transport and Manufacturing, *Cranfield University*, Cranfield, MK43 0AL, United Kingdom
[c] Department of Engineering Sciences and Mathematics, *Luleå University of Technology*, 971 187 Luleå, Sweden
* Corresponding Author

Abstract

The Auroral Acceleration Region (AAR) is a key region in understanding the Magnetosphere-Ionosphere interaction. To understand the physical, spatial and temporal features of the region, multi-point measurements are required. Distributed small-satellite missions such as constellations of multiple nano satellites (for example multi-unit CubeSats) would enable such type of measurements. The capabilities of such a mission will highly depend on the number of satellites – one reason that makes low-cost platforms like CubeSats a very promising choice. In a previous study, the state-of-the-art of miniaturized payloads for AAR measurements was analyzed and evaluated and capabilities of different multi-CubeSat configurations equipped with such payloads in addressing different open questions in AAR were discussed. In this paper the mission analysis and possible mission design, as well as necessary technology developments of such multi-CubeSat mission are identified and presented.

Keywords: Auroral Acceleration Region, Formation Flight, Cube Satellites, Mission Analysis, Orbit Optimisation

1. Introduction

With the introduction of small satellites and the exponential rise of number of CubeSat missions, many space science subjects are considering this advancement as a potential way for mission with lower cost, shorter development time, and in some cases, even better in-situ access to space. Successful CubeSat missions and numerous planned missions demonstrate the potential of these platforms.

Space scientists have been studying the physics of the aurora since the early times of the space age. The colourful auroral emissions are one of the end products of the interaction between the solar wind, the magnetosphere, and the ionosphere. They are caused by the electrons that hit the upper atmosphere after being accelerated by electric fields. Discrete auroral arcs are usually tangential to the constant magnetic latitude circles and have widths of tens of kilometres, spread over thousands of kilometres [1]. Together with these arcs, there are generally upward magnetic Field-Aligned Currents (FACs), quasi-static converging electric potential structures, and upgoing ions, in addition to the downgoing electron beams exciting the atmospheric molecules and atoms, creating the aurora. The region in space where the quasi-static acceleration of charged particles by electric fields occurs is called the Auroral Acceleration Region (AAR) and is located at altitudes of approximately 3000 to 14000 km above the auroral oval.

So far, a few missions have been conducted using nanosatellites for auroral studies, including Munin [2], DICE [3], and RAX [4]. Concept missions for studying the AAR using advanced, conventional satellites have been presented. The four-spacecraft Auroral Cluster mission [5] and the two-spacecraft Alfvén mission [6] considered the mass of each spacecraft of their mission to be about 350 kg. However, there has been no studies attempting to study the AAR using CubeSats, except by Sadeghi and Emami [7] where the state-of-the-art of miniaturized payloads for AAR measurements was evaluated and capabilities of different multi-CubeSat configurations equipped with such payloads in addressing different open questions in AAR were discussed. It was concluded that the miniaturization level of the instruments allows for CubeSats as small as 4-6U to be equipped with electron-, ion-, and magnetic field measurements for effective studies of the region. The CubeSats in the configuration were named EIB as each satellite would be equipped with instruments for measurements on Electrons, Ions, and magnetic fields, B. For more details, a summary of the open questions regarding the AAR, the state-of-the-art of the instruments with respect to the AAR studies, or the capabilities of each n-CubeSat configuration, please see [7].

This paper focuses on the mission analysis of such a multi-CubeSat mission to the AAR. The mission proposed in [7] imposes specific requirements in formation configuration, mutual distances, and eventual alignments among satellites when crossing the AAR. The feasibility and the eventual performance of such a mission strictly depend on the typology and stability properties of the selected orbits. This paper outlines the methodology for selecting orbital parameters by

maximizing the number of passages of the formation in the area of interest for the mission duration as well as evaluates and provides robust solutions against orbital perturbations. The design problem becomes even more complex if deployment, formation stability and keeping, or disposal strategies are taken into account. These issues are also considered in the analysis, and their eventual consequences on the spacecraft design is discussed. As a result, the paper shows a baseline orbit design for such kinds of missions, obtained by trading off different typologies of orbits and eventual manoeuvres to be performed during the mission.

This paper is constructed as follows: After this introduction, in Section 2, the scenario definition is presented. In Section 3, the mission requirements will be discussed. Section 4 is dedicated to defining the AAR as the target region for the mission. In sections 5 and 6, nominal orbit design and satellite formation design are discussed, respectively. Section 7 discusses the satellite disposal, and Section 8 presents the results. Concluding remarks are made in Section 9.

2. Scenario Definition

This section outlines the main assumptions made to define the AAR region of interest for auroral studies and the eventual nominal orbital selection for the mission.

2.1 Coordinate Frames

A J2000 ECI reference frame is used throughout this paper and is referred to as ECI from here after.

Due to the dependence of AAR on Earth's magnetic dipole, a Solar Magnetic (SM) coordinate frame is of importance. A SM coordinate frame is constructed such that the z-axis is parallel to Earth's dipole, the y axis points at dusk and x-axis completes the right-handed coordinate. ILat is defined as the latitude where the field line reaches the surface of Earth [8].

To be able to target a specific region of the auroral zone, one needs to use MLT in addition to ILat. A Geocentric Solar Magnetospheric (GSM) coordinate frame is constructed such that the x-axis points from the centre of Earth to the sun, y-axis perpendicular to Earth's magnetic dipole so that the x-z plane contains the dipole axis, and the z-axis completes the right-handed coordinate frame.

The GSM reference frame is displayed in Fig. 1 with MLT, while the SM reference frame and ILat are displayed in Fig. 2.

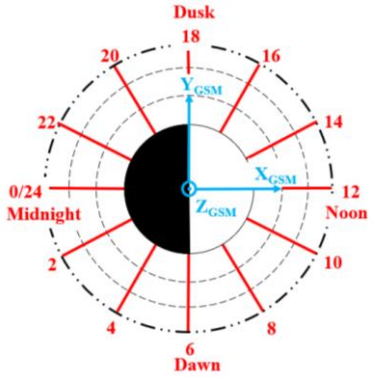

Fig. 1. GSM frame in the ecliptic frame with MLT.

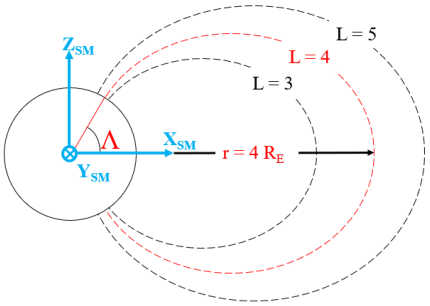

Fig. 2. SM frame in the meridional plane with ILat indicated by Λ.

The GSM and SM reference frames differ by a rotation in the y axis corresponding to the location of the magnetic dipole.

The last coordinate frame of importance is the Local Vertical Local Horizontal (LVLH) coordinate frame attached to the leader satellite. This is constructed by pointing the x-axis along the Earth-leader satellite radius vector, z-axis is perpendicular to the orbital plane and y-axis complete the right-handed coordinate frame. This is shown in Fig. 3.

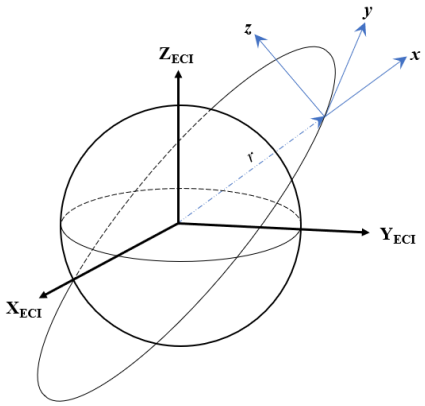

Fig. 3. LVLH coordinate system for relative motion.

2.3 Formation Flight Structure

The satellite formation has been chosen according to [7] to maximise the scientific objectives of this mission

with the formation outlined in Table 1 with respect to the leader EIB1 satellite. This formation only needs to be achieved during the transition through the region of interest in AAR.

Table 1. Formation specification

Satellite	Relative Position
EIB2	(1000km, 0, 0)
EIB3	60s revisit time to EIB1
EIB4	(0, 160km, 0)
EIB5	(-200, 0, 0)
EIB6	60s revisit time to EIB2
EIB7	120s revisit time to EIB1
EIB8	(1200km, 0, 0)
EIB9	(0, -160, 0)

All distances in Table 1 are in the LVLH reference frame defined in Fig. 3. Revisit times are defined as the time taken for a satellite to return to the point in space that another (defined) satellite has visited.

An in-plane and cross-plane visual representation of Table 1 can be seen in Fig. 4 and Fig. 5 respectively.

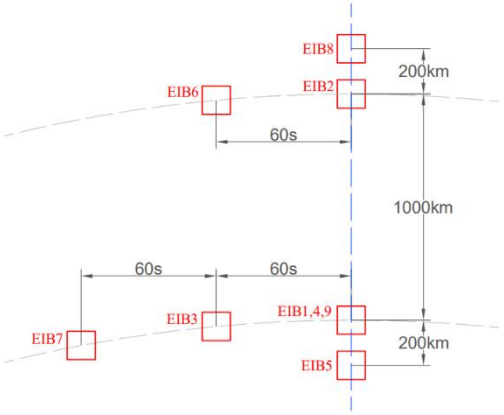

Fig. 4. In-plane orbital view of the satellite formation. Dotted grey lines indicate satellite orbits, while blue show radial line to centre of Earth. The formation is not to scale.

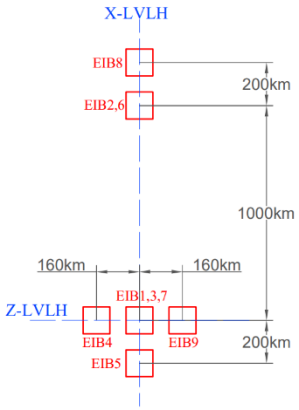

Fig. 5. Cross plane view of the satellite formation. The formation is not to scale.

Table 1, Fig. 4 and Fig. 5 indicate that EIB2, 5 and 8 should be coincident along the LVLH x-axis. This condition is only a first approximate of the instead required condition to be conjugate with EIB1. Satellites are deemed to be conjugate if ΔILat is less than 0.4° [7].

A leader/follower structure is established with EIB1 being the leader, or reference satellite.

3. Mission Requirements

To formalise the mission, a set of high-level mission requirements have been developed based on [7]. These requirements are presented in Tab. 2 below.

Table 2. Mission requirements.

No.	Requirement
M01	The satellites shall pass through the following defined region of AAR over poleward ILat: 65-75° MLT: 19-23hrs Altitude: 6000-8000km
M02	Satellites EIB1-5, 9 shall have at least 20 passages through the region defined by **M01**, of which, 10 are accompanied by EIB7-8 in the formation specified by Table 1 and Fig. 4.
M03	The mission shall conform to space debris mitigation guidelines.
M04	All satellites shall be utilising identical Cubesat platforms.

3.1 Mission duration and end of life

For lower mission costs, in any space mission, the mission lifetime is desired to be as short as possible if the scientific objectives are satisfied. Especially for CubeSats in this study, this is essential to minimize the effects of radiation on the satellites.

The End of Life (EOL) procedures for the satellites include mitigating the spread of debris in space. Typically, this requires either de-orbiting or moving to a graveyard orbit.

4. Definition of the Auroral Acceleration Region

Mission requirement M01 demands a mathematical definition of the concerned region of AAR. To define this specific region, three parameters are needed, the altitude of the region above Earth, the MLT and ILat respectively.

4.1 Magnetic Local Time and Invariant Latitude

An approximation of the MLT of a satellite can be calculated geometrically from the GSM coordinate frame knowing that 15° of longitude is equal to 1 hour of MLT, which follows from

$$MLT = \frac{12}{\pi}\left(\pi + \arctan2\left(\frac{y_{GSM}}{x_{GSM}}\right)\right), \quad (1)$$

where arctan2 is the inverse tangent function defined from -π to π. The ILat of a satellite at some point above Earth is given by

$$\Lambda = \arccos\left(\frac{1}{\sqrt{L}}\right), \quad (2)$$

where L is the McIlwain parameter, or L shell parameter of the magnetic field line measured in Earth radii [9].

To calculate L, a maximum radius approach is used in which the L shell parameter is taken as the maximum distance that the magnetic field line reaches from Earth [10]. To calculate this maximum distance the IGRF13 magnetic field model [11] was used to propagate the magnetic field line associated with specific point in space to its maximum distance from Earth, which in turn gives L.

Based on requirement M01, an ILat range of 65-75° gives a corresponding L shell range of 5.60-14.93 Re.

4.2 Region Definition

Fig. 6 shows the AAR region, along with the highlighted region that is specifically of interest.

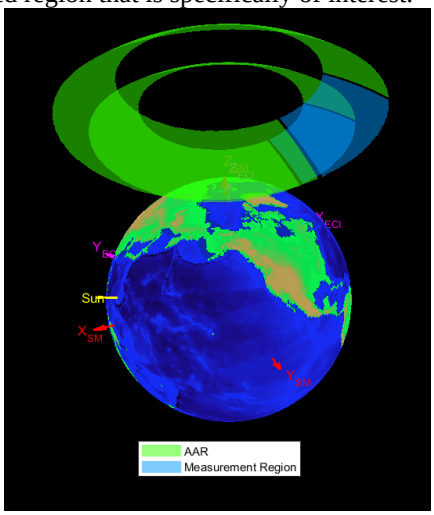

Fig. 6. The green region is AAR above Earth, while the blue sector is the region of AAR that M01 specifies.

This region in Fig. 6 was generated by defining a hemispheric region above Earth and determining the ILat of each point in space, if the points corresponded to the correct ILat they were plotted. This region is not fixed in time. Instead, it has both daily and seasonal variations in its position due to the relationship between ILat and the position of Earth's dipole, and MLT and the position of Earth relative to the Sun.

5. Nominal Orbit Design

To satisfy mission requirement M02, an initial reference orbit is desired that gives the maximum number of crosses of AAR in the fixed mission period of 30-days.

As EIB1 is designated as the reference orbit, this orbit is optimised such that the maximum number of crosses of AAR are achieved. To determine an optimal reference orbit, specific orbital elements are designated as optimisation parameters and optimised through a cost function.

5.1 Optimisation Parameters

To determine which orbital elements i, Ω, ω, f, a and e need to be optimised, physical effects such as J2, solar and drag perturbations, as well as formation periodicity, geometry, and total number of crosses of AAR need to be considered.

The period of an orbit in Keplerian dynamics is wholly dependent on the semi-major axis of that orbit, given by

$$P = 2\pi\sqrt{\frac{a^3}{\mu}}. \quad (3)$$

To ensure formation periodicity in Keplerian dynamics, with satellites acquiring the right configuration when crossing the AAR region, semi-major axis matching is required between satellites due to (3).

This means that for any reference orbit, whether it is circular or eccentric, the follower orbits will have a difference in eccentricity as illustrated in

Fig. 7.

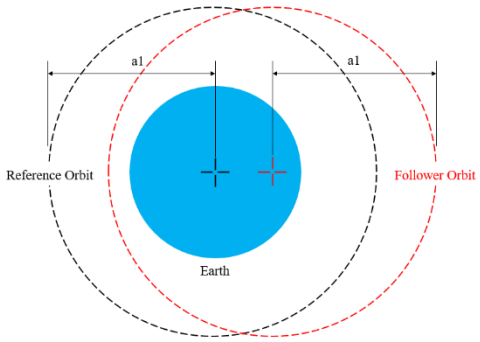

Fig. 7. Reference and follower orbit shifted in eccentricity, but with same semi-major axis a1.

This places restrictions on the minimum altitude of the perigee of the reference orbit and thus the maximum eccentricity of the reference orbit, due to shifting the altitude of the follower orbit higher by 1200km (the

distance that EIB8 is from EIB1), also requires that the perigee is reduced by 1200 km.

Thus, the minimum altitude of the reference orbit must be higher than 1200 km, but additionally as drag effects over a short term are significant at altitudes of 100-400 km [12], a minimum perigee altitude of 1600km for the reference orbit is set such that EIB8 does not orbit lower than 400 km.

With a fixed apogee of 6500 km, this corresponds to a maximum eccentricity of 0.235 for the reference orbit. The inclination is fixed at 90° as polar crosses of AAR are desired. This fixes *i*, giving **Ω**, *e* and ω as optimisation parameters.

5.2 Cost Function

To determine the effect of altering the optimisation parameters to get the maximum number of crosses through AAR possible, a cost function is needed. The selected cost function takes in the initial orbital elements and mission start date, simulates the orbit for the 90-day mission duration and counts the number of times that EIB1 enters the desired area of AAR specified by M01.

The cost function (4) can then be minimised by inverting and squaring the number of crosses to give a total cost based on the initial orbital elements

$$C = \frac{1}{crosses^2} \tag{4}$$

Thus, by increasing the number of crosses of the desired region, the cost function's value will decrease.

6. Satellite Formation Design

To design the orbits of the follower orbits, the differences in the LVLH position and revisit times outlined in Fig. 4 and Table 1 must be considered. It is also required that the formation is regained when transiting through AAR.

6.1 Formation Synchronisation

The formation is synchronised such that it regains its geometry when transitioning through AAR. For an eccentric reference orbit, the formation is synchronised around the apogee of the reference orbit. For a circular reference orbit, the formation is synchronised about the apogee of a higher altitude eccentric follower orbit. This is achieved for an eccentric reference orbit by setting the initial true anomaly to 0° for satellites EIB2, 4, 8, 9 and 180° for EIB5.

However, satellites EIB3, 6, 7 need to have the correct revisit times shown in Fig. 4, and thus required different initial true anomalies. This is determined by utilising Kepler's equation shown in (5).

$$\begin{aligned}\frac{M - M_0}{n} &= t - t_0 \\ &= \sqrt{\frac{a^3}{\mu}}\left[2\pi k + E - e\sin(E) - (E_0 - e\sin E_0)\right]\end{aligned} \tag{5}$$

where *M* is the mean anomaly, *E* is the eccentric anomaly and *n* is the mean orbital motion. This is solved for *E* using the different revisit times and converted into an initial true anomaly angle.

6.2 Designing J2 invariant orbits

Due to J2 perturbations, simply matching the semi-major axis as indicated in

Fig. 7 does not result in the same period. Instead, RAAN, argument of perigee and mean anomaly drift rates differ based on the eccentricity according to (6)-(8) [13],

$$\dot{\Omega} = -\frac{3}{2}J_2 n\left(\frac{R_e}{p}\right)^2 \cos(i) \tag{6}$$

$$\dot{\omega} = \frac{3}{4}J_2 n\left(\frac{R_e}{p}\right)^2 (5\cos^2(i) - 1) \tag{7}$$

$$\dot{M} = n - \frac{3}{2}J_2 n\left(\frac{R_e}{a}\right)^2 \frac{1}{(1-\mathrm{e})^{\frac{3}{2}}}\left(1 - \frac{3}{2}\sin^2(i)\right) \tag{8}$$

where *p* is the semi-latus rectum. (6)-(8) are in terms of mean orbital elements, which ignore small period oscillations. Thus, satellites with different eccentricities will drift apart over time and desynchronise the formation. To mitigate this, two dimensionless constraints with distance normalised by the Earth's radius and μ = 1, defined by (9) and (10) can be constructed such that the relative average drift rate of the angle between the radius vectors are zero [13]. This yields

$$\delta a = \frac{J_2}{2L_0^4\eta_0^5}(4 + 3\eta_0)(1 + 5\cos^2(i_0))L_0\delta\eta \tag{9}$$

$$\delta e = \frac{(1 - e^2)\tan(i)}{4e}\delta i \tag{10}$$

where,

$$\eta = \sqrt{1 - e^2} \tag{11}$$

$$L = \sqrt{\mu a} \tag{12}$$

The nought terms in (9) and (10) refer to the relevant nominal orbit keplerian elements. These constraints place restrictions on the difference between *e*, *i* and *a* of the reference and follower orbits.

However, as the constraint in (10) cannot be fulfilled for every spacecraft that is in plane with EIB1 as there is no difference in inclination. Instead, only (9) can be achieved by altering the semi-major axis and eccentricity to get the desired difference. This means that there will

be a drift between the colatitudes of the reference and follower orbits that may have to be corrected by stationkeeping.

6.3 Formation Performance Verification

To get significant scientific results, the critical factor of mission success is the total number of conjugate crosses achieved, rather than strictly adhering to the defined formation. Thus, to determine the performance of the formation, the conjugacy of EIB2, 5, 6 and 8 is compared against satellites EIB1, 3 and 7.

7. Satellite Deployment & Disposal

To calculate the deployment and disposal Δv costs associated with the chosen orbits for the satellite formation all manoeuvres are assumed to be impulsive.

All satellites are assumed to be within the reference orbit. The deployment of EIB2, 5, 6 and 8 occurs through two impulsive burns to alter the required perigee and apogee altitudes. EIB4 and 9 are deployed by simple inclination changes. Satellites already within the reference orbit have no deployment costs associated with them.

The disposal of the satellites will occur at EOL once the scientific objectives of the mission have been achieved. The satellites will be deorbited using one impulsive burn at apogee to lower the perigee to an altitude such that the satellite deorbits naturally within 25 years.

To calculate the fuel mass costs with these associated manoeuvres, the Tsiolkovsky rocket equation is used.

8. Results

To propagate the orbit, a Matlab implementation of Cowell's method using a RKF78 adaptive step size integrator [14]. The perturbations considered were J2 effects, solar radiation pressure and atmospheric drag. This was compared to STK's HPOP propagator to ensure accuracy of numerical results.

8.1 Nominal Orbit Optimisation

MATLAB was used to optimise the RAAN, argument of perigee and eccentricity using a minimisation pattern search algorithm on (4) for a 30-day mission period. The eccentricity was constrained from 0 to 0.235 which corresponds to a minimum perigee height of 1600km.

This optimisation gave a total of 192 crosses of AAR with the optimisation characteristics shown below.

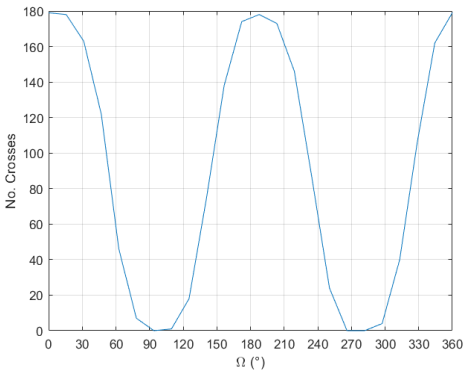

Fig. 8. Number of crosses from optimising RAAN.

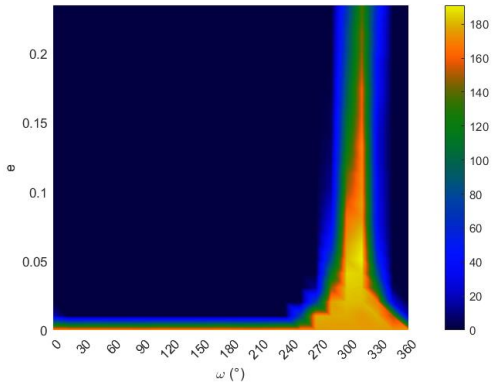

Fig. 9. Optimisation results of argument of perigee and eccentricity.

From Fig. 8, the periodic behaviour of changing the RAAN can be seen, with a maximum of 180 crosses occurring at 0° and 190°. Additionally, for RAAN values that are 90° different to optimal values, there are zero crosses of AAR, which is expected as some orbital planes will not cross through AAR.

Fig. 9 shows that increasing the eccentricity to 0.05, with an argument of perigee of 310° gives 192 crosses of AAR. This increase over RAAN optimisation is due to the reduction in the period of the orbit. However, this also imposes restrictions on the argument of perigee, with the domain of eccentricities and argument of perigee that give nonzero crosses of AAR restricted to a narrow band. This is due to the altitude difference that measurements in AAR are taken at, as the optimisation was aimed at purely 6500km measurements and with a different argument of perigee it changes this altitude.

1.2 Formation Performance

From the nominal orbit selection, an elliptical reference orbit with an eccentricity of 0.05 gives the most crosses of AAR. The total number of conjugate crosses are listed in Table 3.

Table 3. Number of conjugate crosses for the optimised reference orbit

No. Orbits: 192	EIB2	EIB5	EIB6	EIB8
EIB1	127	82	82	122
EIB3	161	30	88	153
EIB7	75	5	106	127

This number of conjugate crosses exceeds mission requirement M02, and thus station keeping is not required to extend the mission duration.

Fig. 10-Fig. 13 shows the evolution of the absolute ΔILat for EIB2, 5, 6 and 8 against EIB1, 3 and 7 across the 30-day mission timeline for the eccentric reference orbit.

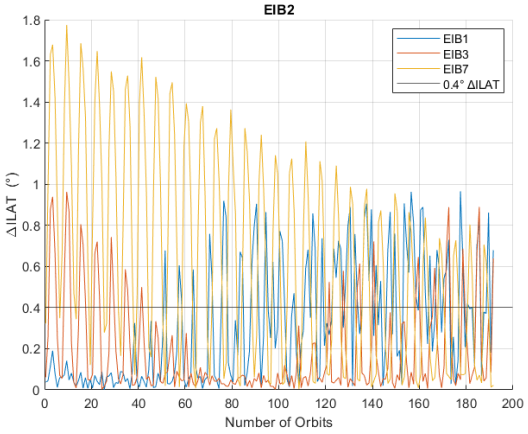

Fig. 10. Absolute ΔILat for EIB2 against EIB1, EIB3 and EIB7.

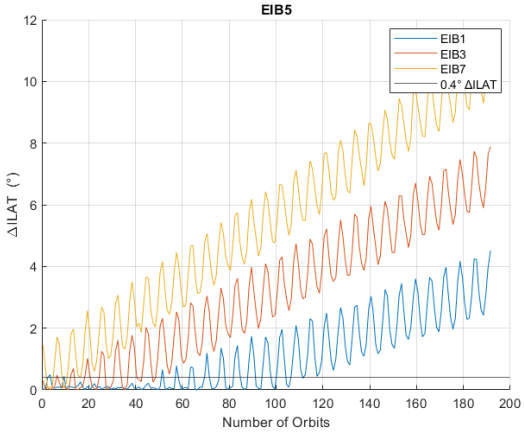

Fig. 11. Absolute ΔILat for EIB5 against EIB1, EIB3 and EIB7.

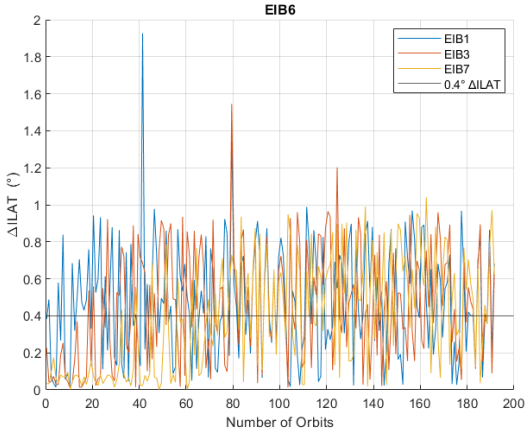

Fig. 12. Absolute ΔILat for EIB6 against EIB1, EIB3 and EIB7.

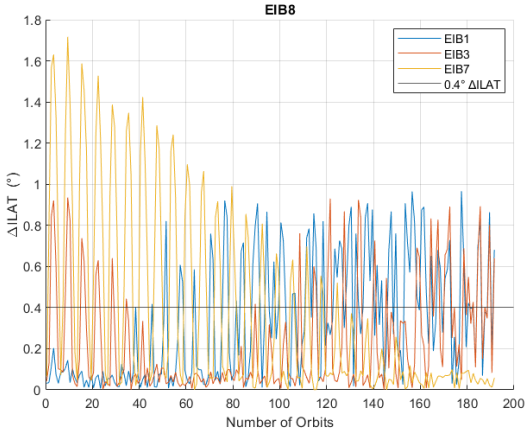

Fig. 13. Absolute ΔILat for EIB8 against EIB1, EIB3 and EIB7.

From Fig. 11 and Fig. 13, both figures demonstrate how satellite EIB2 and EIB8 start conjugate with EIB1 for approximately the first 40 orbits, become conjugate with EIB3 while losing conjugacy with EIB1, and then finally for EIB8 becomes conjugate with EIB7. This transfer in conjugacy for satellites EIB2, 5 6 and 8 from EIB1, to EIB3 and finally EIB7 allows for the mission to continue to function throughout the 30-day timeline.

Additionally, from Fig. 11, EIB5 provides redundancy and verification of measurements for EIB1, loses conjugacy with EIB1 after 105 orbits.

The conjugacy behaviour of satellite EIB6 is difficult to discern, however from Table 3, the total number of conjugate crosses against EIB1 and 3 is similar, with 20 crosses more with EIB7. This is expected as from Fig. 4, EIB6 is situated between EIB1, 3 and 7.

Due to J2 perturbations, there is lagging/procession behaviour in the along-track distance for satellites with different eccentricities due to the mean anomaly rate of change shown by (8).

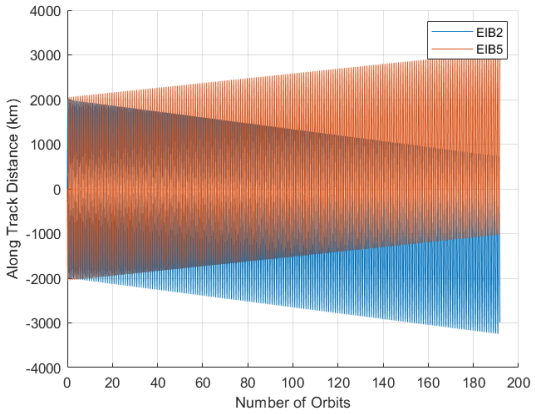

Fig. 14. Along-track distance for EIB2 and EIB5 relative to EIB1 in the LVLH frame.

This lagging/procession behaviour in the along-track distance is demonstrated by Fig. 14 where for EIB2, the along-track distance in the EIB1 LVLH reference frame increases with time, thus transferring its conjugacy to EIB3 and 7 as the mission progresses.

Interestingly, Fig. 14 shows that EIB5 moves opposite to EIB2 in the along-track direction relative to EIB1. This is due to the differing argument of perigee of EIB5, which is flipped 180° relative to EIB2, 6 and 8. The effect of this can be seen in Fig. 11 where EIB3 and 7 do not display the same conjugacy transfer behaviour with EIB5 that EIB2 and 8 experience.

The overall effect of this formation drift due to J2 for can be seen in Fig. 15.

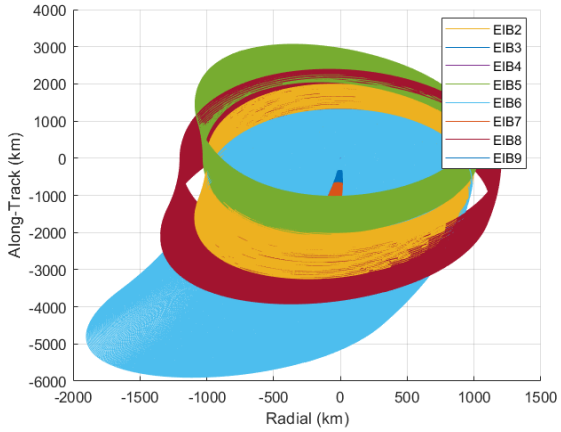

Fig. 15. Overall formation evolution in the x-y LVLH plane.

From Fig. 15, satellites EIB6 experiences the largest deviation from its nominal position, while all other satellites experience some form of deformation.

This change in position is due to both different mean anomaly rates, and argument of perigee rate of change. This means that for a longer mission duration, station keeping will be needed to correct the formation geometry to get valid scientific results. Additionally, out of plane dynamics that EIB4 and 9 experience are negligent to the performance of the satellite formation.

As station keeping is not required, only the deployment and disposal costs need to be calculated.

The satellite is assumed to be a 15 kg dry mass 12U CubeSat with manoeuvres performed by a typical with an I_{sp} of 220s [15]. The fuel costs were calculated such that the deployment fuel mass takes the deorbit fuel and dry mass into account, while the deorbit only the dry mass of the satellite. No fuel costs associated with a phasing plan have been calculated.

Table 4. Total fuel costs where each fuel cost is per satellite in that orbit.

	Deployment Δv (m/s)	Disposal Δv (m/s)	Fuel mass (kg)
Ref. Orbit	0.0	836.2	7.1
EIB2/6	231.1	685.4	7.3
EIB4/9	71.5	836.2	7.6
EIB5	46.5	806.6	7.1
EIB8	277.1	654.5	7.4

Table 4 demonstrates that the wet mass of the satellite, 15 kg + fuel mass, is less than a nominal 12U total weight of 24 kg [16]. Additionally, as the target region of AAR is not a protected region of space [17] and due to the limited number of operational satellites that are present in this orbital region, deorbiting may not be necessary as the risk of collision in this region is extremely low. This would eliminate a large portion of the fuel required leaving only deployment costs. To eliminate propulsion from the CubeSat platform, which is desirable for a cost and complexity point of view, third party deployment mechanisms that deposit the satellites in their required orbits need to be studied and determined if feasible to utilise.

9. Conclusion & Further Studies

This paper has analysed the feasibility of a multiple CubeSat mission to study the auroral acceleration region through determining the region in space that the formation needs to be present in, optimising a nominal orbit that the formation will be defined around and determining properties of the formation orbits to minimise formation drift over the 30 day mission lifetime. It was found that in a 30 day mission timeline with 192 crosses of AAR, while the satellite formation does deteriorate, the scientific objectives of the mission are achieved in a 12U CubeSat platform. Additionally, to eliminate the need for propulsion systems on the satellites, de-orbiting does not need to be attempted due to the target region of AAR not being protected, while

future studies on the feasibility of using third party deployment methods need to be considered. Other nominal orbits such as a circular reference orbit also need to be studied and compared to the optimised reference orbit to see if they generate favourable dynamics that increase the scientific output of the mission,

References

[1] G. Paschmann, S. Haaland, and R. Treumann, Auroral plasma physics, vol. 15. Springer Science & Business Media, 2012.

[2] O. Norberg et al., "The microsatellite ASTRID," 1995.

[3] C. S. Fish et al., "Design, development, implementation, and on-orbit performance of the dynamic ionosphere CubeSat experiment mission," Space Science Reviews, vol. 181, no. 1–4, pp. 61–120, 2014.

[4] H. Bahcivan, J. W. Cutler, J. C. Springmann, R. Doe, and M. J. Nicolls, "Magnetic aspect sensitivity of high-latitude E region irregularities measured by the RAX-2 CubeSat," Journal of Geophysical Research: Space Physics, vol. 119, no. 2, pp. 1233–1249, 2014.

[5] J. Andrews, J. Scherrer, J. Waite, and J. Burch, "Auroral Cluster-A space physics mission for multiple, electronically tethered small satellites," in Space Programs and Technologies Conference, 1991, p. 1567.

[6] M. Berthomier et al., "Alfvén: magnetosphere—ionosphere connection explorers," Experimental Astronomy, vol. 33, no. 2, pp. 445–489, 2012.

[7] S. Sadeghi and M. R. Emami, "Multi-spacecraft studies of the auroral acceleration region: From cluster to nanosatellites," Advances in Space Research, vol. 59, no. 5, pp. 1173–1188, 2017.

[8] M. G. Kivelson, M. G. Kivelson, and C. T. Russell, Introduction to space physics. Cambridge university press, 1995.

[9] C. E. McIlwain, "Magnetic coordinates," Space Science Reviews, vol. 5, no. 5, pp. 585–598, 1966.

[10] J. Pilchowski, A. Kopp, K. Herbst, and B. Heber, "On the definition and calculation of a generalised McIlwain parameter," Astrophysics and Space Sciences Transactions, vol. 6, no. 1, pp. 9–17, 2010.

[11] P. Alken et al., "International geomagnetic reference field: the thirteenth generation," Earth, Planets and Space, vol. 73, no. 1, pp. 1–25, 2021.

[12] D. A. Vallado and D. Finkleman, "A critical assessment of satellite drag and atmospheric density modeling," Acta Astronautica, vol. 95, pp. 141–165, 2014.

[13] K. T. Alfriend and H. Schaub, "Dynamic and control of spacecraft formations: challenges and some solutions," The Journal of the Astronautical Sciences, vol. 48, no. 2, pp. 249–267, 2000.

[14] D. A. Vallado, Fundamentals of astrodynamics and applications, vol. 12. Springer Science & Business Media, 2001.

[15] "https://nanoavionics.com/," Nano Avionics, [Online]. Available: https://nanoavionics.com/. [Accessed 09 20 2021].

[16] A. Johnstone, "CubeSat Design Specification (1U-12U) REV 14," Cal Poly, San Luis Obispo, CA, 2020.

[17] M. Yakovlev, "The 'IADC Space Debris Mitigation Guidelines' and supporting documents," in 4th European Conference on Space Debris, 2005, vol. 587, pp. 591–597.

2021-10-25

Multi-Cubesat mission for auroral acceleration region studies

Castro, Marley

International Astronautical Federation